Supporting Information

On the Antitumor Properties of Novel Cyclometalated Benzimidazole Ru(II), Ir(III) and Rh(III) Complexes

Gorakh S. Yellol,[a] Antonio Donaire,[a] Jyoti G. Yellol,[a] Vera Vasylyeva,[b]

Christoph Janiak,[b] and José Ruiz[a] *

[a]Departamento de Química Inorgánica and Regional Campus of International Excellence "Campus Mare Nostrum", Universidad de Murcia and Instituto Murciano de Investigación Biosanitaria,Murcia, Spain. Fax: 34 868884148; Tel: 34 868887477; E-mail: jruiz@um.es; [b]Institut für Anorganische Chemie und Strukturchemie Universität Düsseldorf, D-40204 Düsseldorf, Germany

Table of Contents

General

The C, H, and N analyses were performed with a Carlo Erba model EA 1108 microanalyzer. The ^{1}H and ^{13}C NMR spectra were recorded on a Bruker AC 300E or a Bruker AV 400 spectrometer. Chemical shifts are cited relative to $SiMe_4$ (^{1}H and ^{13}C, external). ESI mass (positive mode) analyses were performed on a HPLC/MS TOF 6220. UV/vis spectroscopy was carried out on a Perkin Elmer Lambda 750 S spectrometer with operating software. Fluorescence measurements were carried out with a Perkin Elmer LS 55 50 Hz Fluorescence Spectrometer.

Solvents were dried by the usual methods. $[(\eta^6\text{-cymene})RuCl_2]_2$, $[(\eta^5\text{-}C_5Me_5)MCl_2]_2$ (M = Rh and Ir), sodium salt of calf thymus DNA, ethidium bromide (EB), Hoechst 33258, human serum albumin (HSA) were obtained from Sigma-Aldrich (Madrid, Spain); pB*R*322 plasmid DNA used in the studies were obtained from Boehringer-Mannheim (Mannheim, Germany).

Preparation and Characterization of Compounds 1-11

Compound **1**

Methyl 4-fluoro-3-nitrobenzoate (1 mmol) was dissolved in dichloromethane (10 mL) in round

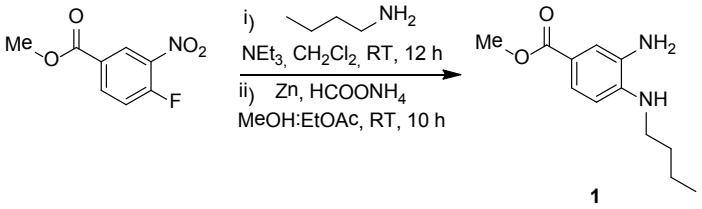

1

bottom flask equipped with stirrer and nitrogen atmosphere. Butyl amine (2 mmol) was added to it at room temperature with constant stirring followed by addition of triethyl amine (2 mmol). The reaction mixture was stirred at room temperature for 12 h and the progress of reaction was monitored by TLC. After complete conversion, reaction was quenched by water (10 mL) and product was extracted by dichloromethane (2 × 10 mL). The combined dichloromethane layer was washed with water (10 mL) and brine (10 mL), dried on sodium sulfate and concentrated under reduced pressure. The crude product was purified by column chromatography using ethyl acetate-hexane (1:5) as eluent to get methyl 4-(butylamino)-3-nitrobenzoate in 79% yield. Subsequently, methyl 4-(butylamino)-3-nitrobenzoate (1 mmol) was dissolved in methanol (10 mL) in round bottom flask equipped with stirrer and nitrogen atmosphere. Zinc (3 mmol) was added at room temperature with constant stirring followed by addition of ammonium format (2 mmol) in two batches. The reaction mixture was stirred at room temperature for 5 h and the progress of reaction was monitored by TLC. After complete conversion, reaction was filtered to remove zinc and unreacted ammonium formate. Filtrate was concentrated and then dissolved in dichloromethane and stirred for 30 min. The undissolved material was removed by filtration and dichloromethane was concentrated under reduced pressure. The crude product was purified by column

chromatography using ethyl acetate-hexane (1:2) as eluent to get methyl 3-amino-4-(butylamino)benzoate (**1**) in 68% yield.

Compounds **2**

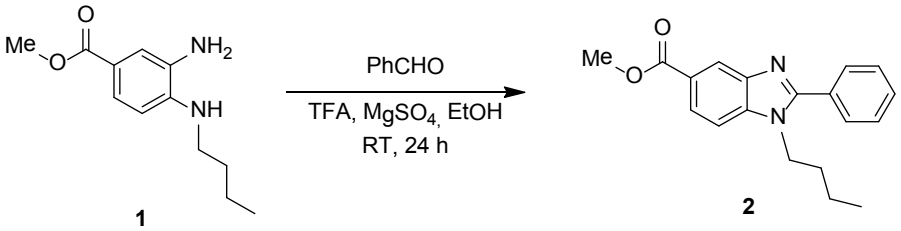

1 **2**

Methyl 3-amino-4-(butylamino)benzoate **1** (1 mmol) was dissolved in ethanol (10 mL) in round bottom flask equipped with stirrer and nitrogen atmosphere. Benzaldehyde (1.2 mmol) was added at room temperature with constant stirring followed by addition of trifluoroacetic acid (0.1 mmol) and magnesium sulfate (5 mmol). The reaction mixture was stirred at room temperature for 24h and the progress of reaction was monitored by TLC. After complete conversion, reaction was filtered to remove magnesium sulfate. Filtrate was concentrated and then dissolved in dichloromethane. Dichloromethane was washed with water (2 x 10 mL) and brine (10 mL), dried on sodium sulfate and concentrated under reduced pressure. The crude product was purified by column chromatography using ethyl acetate-hexane (1:3) as eluent to obtain methyl 1-butyl-2-phenyl-1*H*-benzimidazole-5-carboxylate (**2**) in 57% yield. ^{1}H NMR (400.13 MHz, $CDCl_3$) δ 8.54 (d, J = 1.4 Hz, 1H), 8.06 (dd, J = 8.5, 1.4 Hz, 1H), 7.73 (m, 2H), 7.54 (m, 3H), 7.45 (d, J = 8.5 Hz, 1H), 4.26 (t, J = 7.6 Hz, 2H), 3.95 (s, 3H), 1.80 (quint, J = 7.5 Hz, 2H), 1.28 (sext, J = 7.5 Hz, 2H), 0.86 (t, J = 7.4 Hz, 3H) ppm; ^{13}C NMR (100.60 MHz, $CDCl_3$) δ 167.6, 155.4, 142.6, 138.8, 130.1, 130.0, 129.2, 128.7, 124.4, 124.1, 122.2, 109.7, 52.0, 44.6, 31.7, 19.8, 13.4; ppm; MS (ESI-MS) Z = 309 $(M+H)^+$; Anal. Calcd for $C_{19}H_{20}N_2O_2$ (308,37): C, 74.00; H, 6.54; N, 9.08; Found: C, 73.72; H, 6.56; N, 8.87 (%).

Compound **3**

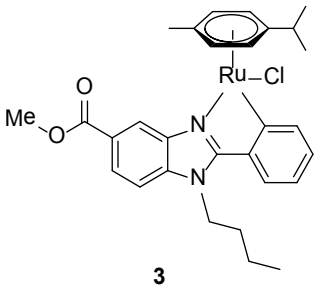

3

Methyl 1-butyl-2-phenyl-1*H*-benzimidazole-5-carboxylate **2** (1 mmol) was dissolved in freshly distilled dichloromethane in dry round bottom flask equipped with stirrer and nitrogen atmosphere. Sodium acetate (1.2 mmol) was added in it at room temperature with constant stirring followed by

addition of $[(\eta^6\text{-cymene})RuCl_2]_2$ (0.5 mmol). The reaction mixture was stirred at room temperature for 12h and the progress of reaction was monitored by TLC. After complete conversion, dichloromethane was removed under reduced pressure and diethyl ether (10 mL) was added in it. Reaction mixture was stirred for 10 min, product was precipitate out. The crystalline product was filtered through G4 filtration funnel and dried well. The reddish brown colored ruthenium complex **3** was obtained in good yield (60%). ^{1}H NMR (600.13 MHz, $CDCl_3$) δ 8.64 (d, *J* = 1.4 Hz, 1H), 8.35 (dd, *J* = 7.6, 1.0 Hz, 1H), 8.03 (dd, *J* = 8.5, 1.4 Hz, 1H), 7.64 (d, *J* = 7.6 Hz, 1H), 7.37 (d, *J* = 8.5 Hz, 1H), 7.23 (dt, *J* = 7.5, 1.0 Hz, 1H), 7.07 (dt, *J* = 7.5, 1.0 Hz, 1H), 5.90 (d, *J* = 5.9 Hz, 1H), 5.74 (d, *J* = 5.9 Hz, 1H), 5.37 (d, *J* = 5.9 Hz, 1H), 5.13 (d, *J* = 5.9 Hz, 1H), 4.48 (m, 1H), 4.37 (m, 1H), 4.02 (s, 3H), 2.31 (m, 1H), 2.10 (s, 3H), 1.90 (quint, *J* = 7.5 Hz, 2H), 1.44 (m, 2H), 0.96 (t, *J* = 7.4 Hz, 3H), 0.95 (d, *J* = 7.0 Hz, 3H), 0.78 (d, *J* = 7.0 Hz, 3H) ppm; ^{13}C NMR (150.89 MHz, $CDCl_3$) δ 184.6, 167.1, 159.5, 140.9, 140.7, 139.2, 133.3, 129.1, 125.2, 124.5, 124.3, 122.6, 119.2, 109.6, 101.2, 99.6, 89.4, 89.1, 82.1, 81.2, 52.2, 44.9, 31.6, 30.8, 22.4, 21.7, 20.1, 18.9, 13.7 ppm; MS (ESI-MS) *Z* = 579 $(M+H)^+$; Anal. Calcd for $C_{29}H_{33}ClN_2O_2Ru$ (578,11): C, 60.25; H, 5.75; N, 4.85; Found: C, 59.94; H, 5.68; N, 4.75 (%).

Compound **4**

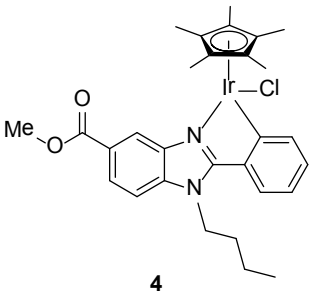

4

Methyl 1-butyl-2-phenyl-1*H*-benzimidazole-5-carboxylate **2** (1 mmol) was dissolved in freshly distilled dichloromethane in dry round bottom flask equipped with stirrer and nitrogen atmosphere. Sodium acetate (1.2 mmol) was added in it at room temperature with constant stirring followed by addition of $[(\eta^5\text{-}C_5Me_5)IrCl_2]_2$ (0.5 mmol). The reaction mixture was stirred at room temperature for 12h. After complete conversion, dichloromethane was removed under reduced pressure and product was precipitate by addition of diethyl ether (10 mL) with constant stirring. The crystalline product was filtered and dried well. The yellow colored iridium complex **4** was obtained in good yield (87%). ^{1}H NMR (400.13 MHz, $CDCl_3$) δ 8.44 (d, *J* = 1.5 Hz, 1H), 8.03 (d, *J* = 7.5 Hz, 1H), 8.00 (dd, *J* = 8.5, 1.5 Hz, 1H), 7.67 (d, *J* = 7.5 Hz, 1H), 7.38 (d, *J* = 8.5 Hz, 1H), 7.21 (dt, *J* = 7.5, 1.0 Hz, 1H), 7.08 (t, *J* = 7.5, 1.0 Hz, 1H), 4.53 (m, 1H), 4.44 (m, 1H), 3.97 (s, 3H), 1.99 (quint, *J* = 7.5 Hz, 2H), 1.78 (s, 15H), 1.51 (m, 2H), 1.00 (t, *J* = 7.4 Hz, 3H) ppm; ^{13}C NMR (100.60 MHz, $CDCl_3$) δ 167.1, 166.3, 163.6, 139.3, 139.2, 137.1, 133.5, 130.9, 125.1, 124.4, 124.0, 122.0, 119.0, 109.8, 88.3, 52.1, 44.9, 31.8, 20.2, 13.7, 9.7 ppm; MS (ESI-MS) *Z* =

635 $(M\text{-}Cl)^+$; Anal. Calcd for $C_{29}H_{34}ClN_2O_2Ir$ (670,26): C, 51.97; H, 5.11; N, 4.18; Found: C, 51.84; H, 5.07; N, 4.20 (%).

Compound **5**

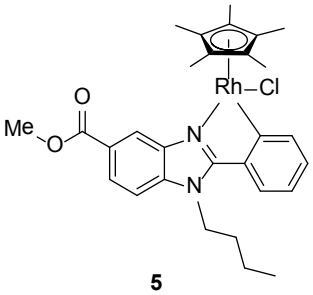

5

Methyl 1-butyl-2-phenyl-1*H*-benzimidazole-5-carboxylate **2** (1 mmol) was dissolved in freshly distilled dichloromethane in dry round bottom flask equipped with stirrer and nitrogen atmosphere. Sodium acetate (1.2 mmol) was added in it at room temperature with constant stirring followed by addition of $[(\eta^5\text{-}C_5Me_5)RhCl_2]_2$ (0.5 mmol). The reaction mixture was stirred at room temperature for 12h. Dichloromethane was removed under reduced pressure and product was precepited in diethyl ether (10 mL). The crystalline product was filtered and dried well. The yellow colored rhodium complex **5** obtained in good yield (60%). ^{1}H NMR (400 MHz, $CDCl_3$) δ 8.51 (d, *J* = 1.3 Hz, 1H), 8.02 (dd, *J* = 8.5, 1.3 Hz, 1H), 8.01 (dd, *J* = 7.5, 1.0 Hz, 1H), 7.63 (d, *J* = 7.7, 1.0 Hz, 1H), 7.39 (d, *J* = 8.5 Hz, 1H), 7.29 (dd, *J* = 7.5, 1.1 Hz, 1H), 7.11 (dt, *J* = 7.5, 1.0 Hz, 1H), 4.48 (m, 2H), 3.97 (s, 3H), 1.98 (quint, *J* = 7.5 Hz, 2H), 1.70 (s, 15H), 1.52 (m, 2H), 1.03 (t, *J* = 7.4 Hz, 3H) ppm; ^{13}C NMR (100 MHz, $CDCl_3$) δ 166.7, 166.2, 163.3, 139.0, 138.1, 136.7, 133.2, 130.4, 124.9, 124.2, 123.9, 121.8, 118.7, 109.6, 88.1, 51.8, 44.6, 31.7, 20.0, 13.4, 9.5 ppm; MS (ESI-MS) *Z* = 545 $(M\text{-}Cl)^+$; Anal. Calcd for $C_{29}H_{34}ClN_2O_2Rh$ (580,95): C, 59.96; H, 5.90; N, 4.82; Found: C, 59.75; H, 5.79; N, 4.69 (%).

Compound **6**

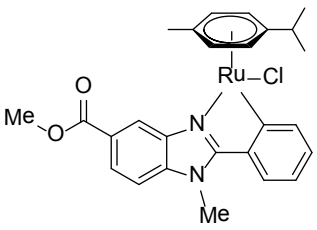

6

Compound **6** was synthesized using similar procedure for synthesis of compound **3**.

^{1}H NMR (300.13 MHz, $CDCl_3$) δ 8.64 (d, *J* = 1.4 Hz, 1H), 8.35 (d, *J* = 7.5 Hz, 1H), 8.03 (dd, *J* = 8.5, 1.4 Hz, 1H), 7.76 (dd, *J* = 7.6, 1.0 Hz, 1H), 7.38 (d, *J* = 8.5 Hz, 1H), 7.22 (dt, *J* = 7.4, 1.0 Hz, 1H), 7.05 (dt, *J* = 7.4, 1.0 Hz, 1H), 5.88 (d, *J* = 5.9 Hz, 1H), 5.78 (d, *J* = 5.9 Hz, 1H), 5.38 (d, *J* = 5.9 Hz, 1H), 5.13 (d, *J*

= 5.9 Hz, 1H), 4.04 (s, 3H), 4.02 (s, 3H), 2.36 (m, 1H), 2.07 (s, 3H), 0.97 (d, J = 6.9 Hz, 3H), 0.82(d, J = 6.9 Hz, 3H) ppm; ^{13}C NMR (75.43 MHz, $CDCl_3$) δ 178.0, 168.0, 161.0, 141.8, 141.5, 140.3, 134.4, 130.1, 126.0, 125.5, 125.4, 123.4, 119.9, 110.4, 101.6, 101.1, 90.3, 89.6, 82.7, 82.0, 53.1, 33.3, 31.7, 23.3, 22.8, 19.8 ppm; MS (ESI-MS) Z = 537 $(M+H)^+$; Anal. Calcd for $C_{26}H_{27}ClN_2O_2Ru$ (536,03): C, 58.26; H, 5.08; N, 5.23; Found: C, 58.14; H, 5.17; N, 5.31 (%).

Compound **7**

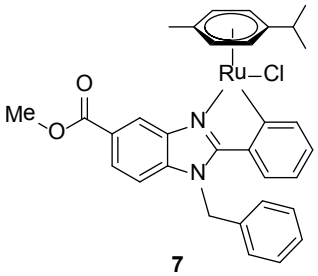

7

Compound **7** was synthesized using similar procedure for synthesis of compound **3**.
^{1}H NMR (400.13 MHz, $CDCl_3$) δ 8.69 (d, J = 1.4 Hz, 1H), 8.33 (dd, J = 7.5, 0.9 Hz, 1H), 8.01 (dd, J = 8.5, 1.4 Hz, 1H), 7.50 (dd, J = 7.7, 0.9 Hz, 1H), 7.33 (d, J = 8.5 Hz, 1H), 7.28 (m, 3H), 7.17 (dt, J = 7.5, 1.0 Hz, 1H), 7.08 (m, 2H), 6.92 (dt, J = 7.5, 1.0 Hz, 1H), 5.95 (d, J = 5.9 Hz, 1H), 5.77 (d, J = 17.5 Hz, 1H), 5.73 (d, J = 5.9 Hz, 1H), 5.63 (d, J = 17.5 Hz, 1H), 5.45 (d, J = 5.9 Hz, 1H), 5.17 (d, J = 5.9 Hz, 1H), 4.02 (s, 3H), 2.32 (m, 1H), 2.13 (s, 3H), 0.95 (d, J = 6.9 Hz, 3H), 0.80(d, J = 6.9 Hz, 3H) ppm; ^{13}C NMR (100.60 MHz, $CDCl_3$) δ 167.8, 167.2, 165.3, 140.4, 140.3, 137.8, 135.8, 134.0, 131.9, 130.1(2C), 129.0, 126.7(2C), 126.4, 125.6, 125.3, 122.9, 119.9, 110.8, 89.2(5C), 53.0, 49.3, 10.6(5C) ppm; MS (ESI-MS) Z = 613 $(M+H)^+$; Anal. Calcd for $C_{32}H_{31}ClN_2O_2Ru$ (612,12): C, 62.79; H, 5.10; N, 4.58; Found: C, 62.71; H, 5.19; N, 4.50 (%).

Compound **8**

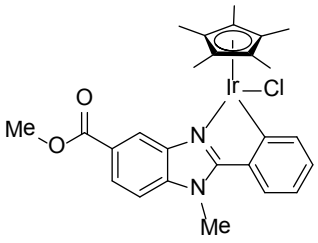

8

Compound **8** was synthesized using similar procedure for synthesis of compound **4**.
^{1}H NMR (400.13 MHz, $CDCl_3$) δ 8.45 (d, J = 1.3 Hz, 1H), 8.00 (m, 2H), 7.80 (dd, J = 7.8, 1.0 Hz, 1H), 7.37 (d, J = 8.5 Hz, 1H), 7.22 (dt, J = 7.5, 1.1 Hz, 1H), 7.06 (dt, J = 7.5, 1.1 Hz, 1H), 7.32 (m, 4H), 7.16 (m, 3H), 6.93 (dd, J = 7.5, 1.1 Hz, 1H), 6.91 (dd, J = 7.5, 1.1 Hz, 1H), 4.13 (s, 3H), 3.97 (s, 3H), 1.79 (s, 15H) ppm; ^{13}C NMR (100.60 MHz, $CDCl_3$) δ 167.0, 166.0, 164.2, 139.4, 139.2, 136.9, 133.8, 131.0,

125.1, 124.5, 124.4, 122.0, 118.9, 109.6, 88.2, 52.1, 32.1, 9.7 ppm; MS (ESI-MS) Z = 593 $(M–Cl)^+$; Anal. Calcd for $C_{26}H_{28}ClN_2O_2Ir$ (628.18): C, 49.71; H, 4.49; N, 4.46; Found: C, 49.47; H, 4.69; N, 4.42 (%).

Compound **9**

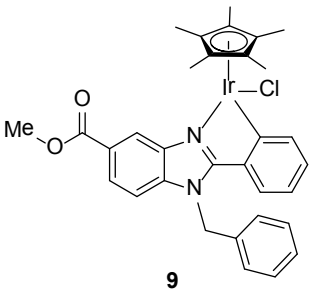

9

Compound **9** was synthesized using similar procedure for synthesis of compound **4**.
^{1}H NMR (400.13 MHz, $CDCl_3$) δ 8.50 (d, J = 1.5 Hz, 1H), 8.01 (dd, J = 7.7, 0.9 Hz, 1H), 7.98 (dd, J = 8.5, 1.5 Hz, 1H), 7.54 (dd, J = 7.9, 0.9 Hz, 1H), 7.32 (m, 4H), 7.16 (m, 3H), 6.93 (dd, J = 7.9, 1.0 Hz, 1H), 6.91 (dd, J = 7.9, 1.0 Hz, 1H), 5.79 (d, J = 17.5 Hz, 1H), 5.70 (d, J = 17.5 Hz, 1H), 3.97 (s, 3H), 1.80 (s, 15H) ppm; ^{13}C NMR (150.89 MHz, $CDCl_3$) δ 167.0, 166.0, 164.2, 139.4, 139.2, 136.9, 133.8, 131.0, 125.1, 124.5, 124.4, 122.0, 118.9, 109.6, 88.2, 52.1, 32.1, 9.7 ppm; MS (ESI-MS) Z = 669 $(M–Cl)^+$; Anal. Calcd for $C_{32}H_{32}ClN_2O_2Ir$ (704.27): C, 54.57; H, 4.58; N, 3.98; Found: C, 54.42; H, 4.54; N, 4.02 (%).

Compound **10**

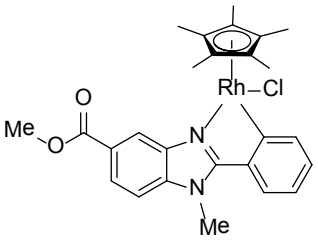

10

Compound **10** was synthesized using similar procedure for synthesis of compound **5**.
^{1}H NMR (300.13 MHz, $CDCl_3$) δ 8.52 (d, J = 1.4 Hz, 1H), 8.02 (d, J = 7.6 Hz, 1H), 8.01 (dd, J = 8.5, 1.4 Hz, 1H), 7.74 (d, J = 7.7, 1.1 Hz, 1H), 7.38 (d, J = 8.5 Hz, 1H), 7.29 (dt, J = 7.5, 1.1 Hz, 1H), 7.11 (dt, J = 7.5, 1.1 Hz, 1H), 4.08 (s, 3H), 3.98 (s, 3H), 1.71 (s, 15H) ppm; ^{13}C NMR (75.43 MHz, $CDCl_3$) δ 167.1, 139.7, 139.6, 137.7, 134.3, 130.2, 129.4, 128.7, 125.0, 124.3, 124.2, 122.7, 119.3, 109.6, 95.9, 95.8, 52.1, 32.3, 9.8, 9.3 ppm; MS (ESI-MS) Z = 503 $(M–Cl)^+$; Anal. Calcd for $C_{26}H_{28}ClN_2O_2Rh$ (538.87): C, 57.95; H, 5.24; N, 5.20; Found: C, 57.64; H, 5.02; N, 5.04 (%).

Compound **11**

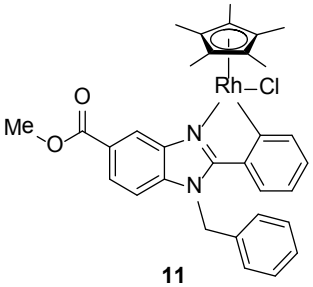

11

Compound **11** was synthesized using similar procedure for synthesis of compound **5**.

^{1}H NMR (400.13 MHz, $CDCl_3$) δ 8.57 (d, J = 1.2 Hz, 1H), 8.00 (m, 2H), 7.49 (dd, J = 7.8, 1.1 Hz, 1H), 7.34 (m, 4H), 7.22 (dd, J = 7.6, 1.1 Hz, 1H), 7.16 (d, J = 7.4, 1.1 Hz, 2H), 6.96 (dt, J = 7.5, 1.1 Hz, 1H), 5.77 (d, J = 17.5 Hz, 1H), 5.70 (d, J = 17.5 Hz, 1H), 3.98 (s, 3H), 1.72 (s, 15H) ppm; ^{13}C NMR (100.60 MHz, $CDCl_3$) δ 167.2, 166.1, 164.0, 139.3, 139.0, 136.7, 133.5, 130.8, 124.9, 124.2, 124.0, 121.9, 118.7, 109.4, 88.1, 51.9, 31.9, 9.6 ppm; MS (ESI-MS) Z = 579 $(M–Cl)^{+}$; Anal. Calcd for $C_{32}H_{32}ClN_2O_2Rh$ (614.96): C, 62.50; H, 5.24; N, 4.56; Found: C, 62.36; H, 5.16; N, 4.45 (%).

X-ray Crystallographic Analysis

Compound **4** crystallizes as needles or perhaps more appropriate as long blocks (Fig. S1)

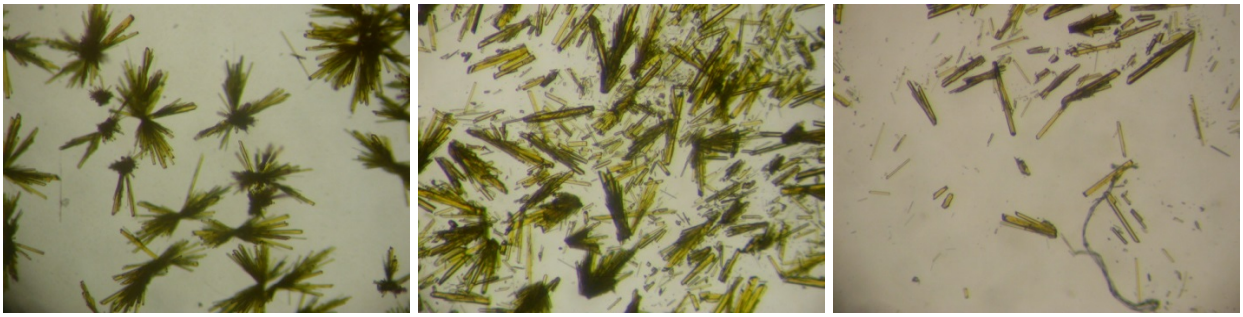

Figure S1. Photographs of crystals of compound **4**.

Suitable single crystals were carefully selected under a polarizing microscope and mounted on a loop. *Data collection*: Compound **4**: Bruker APEX2 CCD diffractometer (with microfocus tube) at 95 ± 2 K; Cu–Kα radiation (λ=1.54178 Å), multilayered mirror system, ω- and ϕ-scan; data collection with Apex2,[i] cell refinement and data reduction with SAINT,[i] experimental absorption correction with SADABS.[ii] *Structure Analysis and Refinement*: The structures were solved by direct methods using SHELXS-97; refinement was done by full-matrix least squares on F^2 using the SHELXL-97 program suite.[iii] All non-hydrogen positions were refined with anisotropic displacement parameters. Hydrogen atoms were positioned geometrically (C---H = 0.95 Å for aromatic CH, C---H = 0.99 Å for CH_2, C---H = 0.98 Å for CH_3) and refined using riding models with $U_{iso}(H) = 1.2\ U_{eq}(CH, CH_2)$ and $U_{iso}(H) = 1.5\ U_{eq}(CH_3)$.

Crystal data and details on the structure refinement are given in Table S1. Graphics were drawn with DIAMOND.[iv] The structural data have been deposited with the Cambridge Crystallographic Data Center (CCDC-No. 950001).

Crystal data and structure refinement for compound 4

Table S1. Crystal data and structure refinement for compound **4**.

Empirical formula	$C_{29}H_{34}ClIrN_2O_2$
M / g mol^{-1}	670.25
Crystal size / mm^3	0.095 × 0.038 × 031
Temperature / K	95(2)
θ range / °(completeness)	4.23-65.95 (94.5%)
h; k; l range	–14, 8; ±16; –18, 17;
Crystal system	Orthorhombic
Space group	$P\,2_12_12_1$
a /Å	12.1557(7)
b /Å	14.0158(8)
c /Å	15.6731(9)
α /°	90
β /°	90
γ /°	90
V /Å^3	2670.3(3)
Z	4
D_{calc}/g cm^{-3}	1.667
μ (Mo Kα) / mm^{-1}	10.819
F(000)	1328
Max./min. transmission	0.7527 / 0.5002
Reflections collected	13015
Independent reflect. (R_{int})	4312 (0.0420)
Data / restraints / parameters	4312 / 0 / 331
Max. / min. $\Delta\rho$ / e.Å^{-3} [a]	1.362 / –1.026
$R1/wR2$ [$I > 2\sigma(I)$] [b]	0.0302 / 0.0653
$R1/wR2$ (all data) [b]	0.0323 / 0.0663
Goodness-of-fit on F^2 [c]	1.109
Flack parameter [d]	0.00

[a] Largest difference peak and hole. – [b] $R_1 = [\Sigma(\|F_o\| - |F_c|)/\Sigma|F_o|]$; $wR_2 = [\Sigma\,[w(F_o^2 - F_c^2)^2]/\Sigma[w(F_o^2)^2]]^{1/2}$. – [c] Goodness-of-fit = $[\Sigma\,[w(F_o^2 - F_c^2)^2]\,/(n-p)]^{1/2}$. – [d] Absolute structure parameter.[v] The compound crystallizes in the orthorhombic non-centrosymmetric space group $P2_12_12_1$ as a racemic twin (BASF scale factor 0.54; the Flack value of 0.00 is meaningless). This means that the structure contains both *R* and *S* configured molecules (enantiomers). The Ir atom in the molecule is a chiral-at-atom center with four different ligands or ligating atoms.

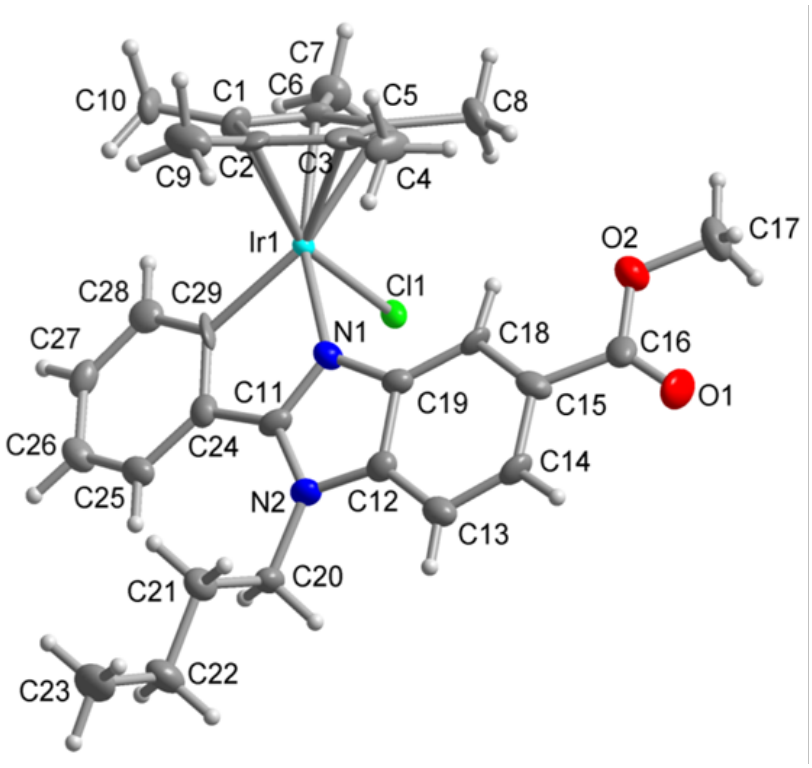

Figure S2. X-ray crystallographic ORTEP diagram of complex **4**

Table S2. Selected distances (Å) and angles (°) for complex **4**.

Atom	Distance to metal (Å)	Atoms of the angle	Angle (°)
Ir1 N1	2.052(5)	N1 Ir1 C29	75.9(2)
Ir1 C29	2.068(5)	N1 Ir1 Cl1	84.31(13)
Ir1 C1	2.166(6)	C29 Ir1 Cl1	89.26(14)
Ir1 C2	2.163(5)	N1 Ir1 Cp(centroid)	133.97(13)
Ir1 C3	2.243(5)	Cl1 Ir1 Cp(centroid)	122.821(82)
Ir1 C5	2.247(5)	C29 Ir1 Cp(centroid)	133.49(14)
Ir1 C6	2.177(5)		
Ir1 Cl1	2.4050(11)		
Ir1 Cp(centroid)	1.828(6)		

COSY, NOESY experiments of Compound 3, 4, 5:

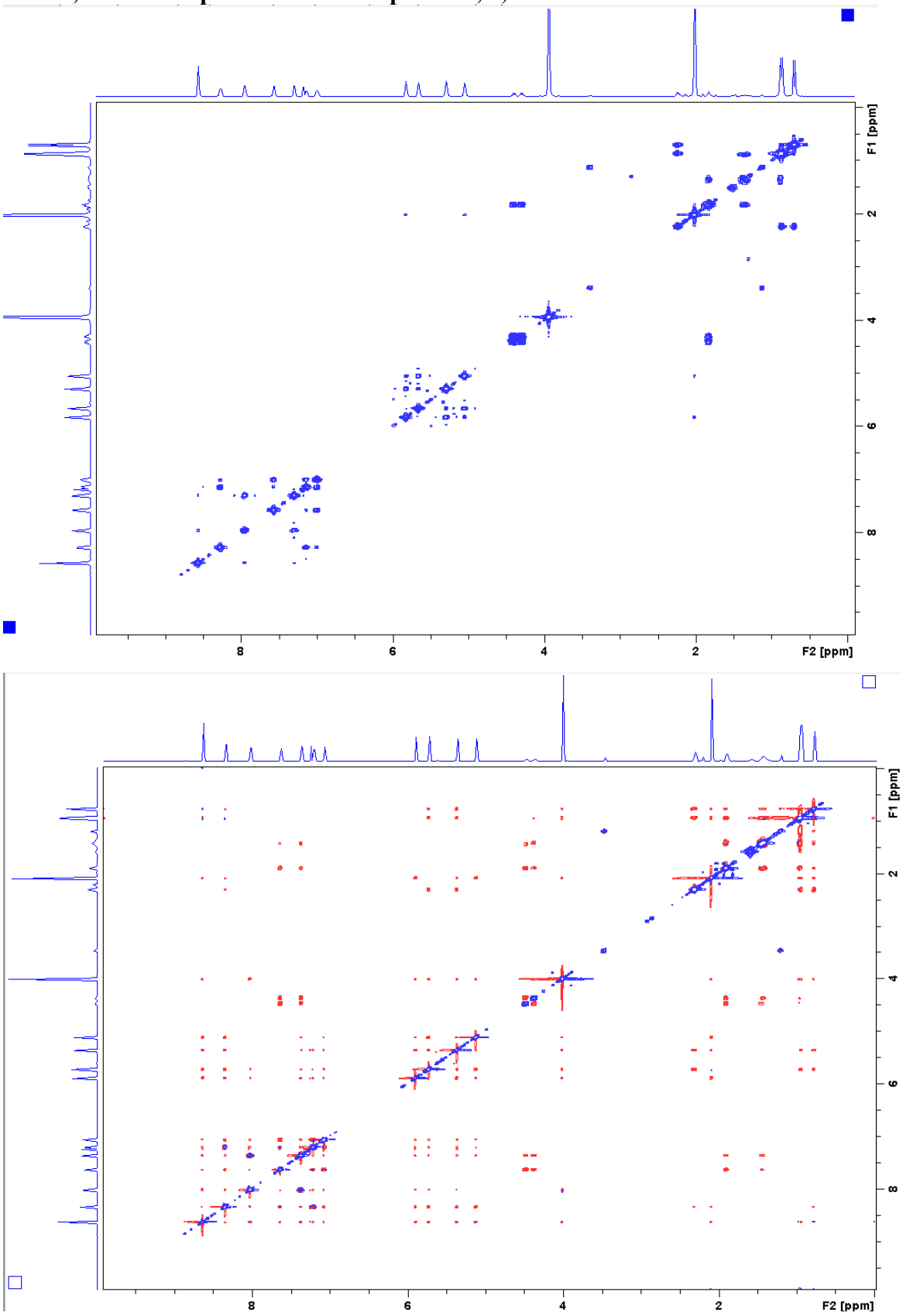

Figure S3. COSY and NOESY spectra for compound **3.**

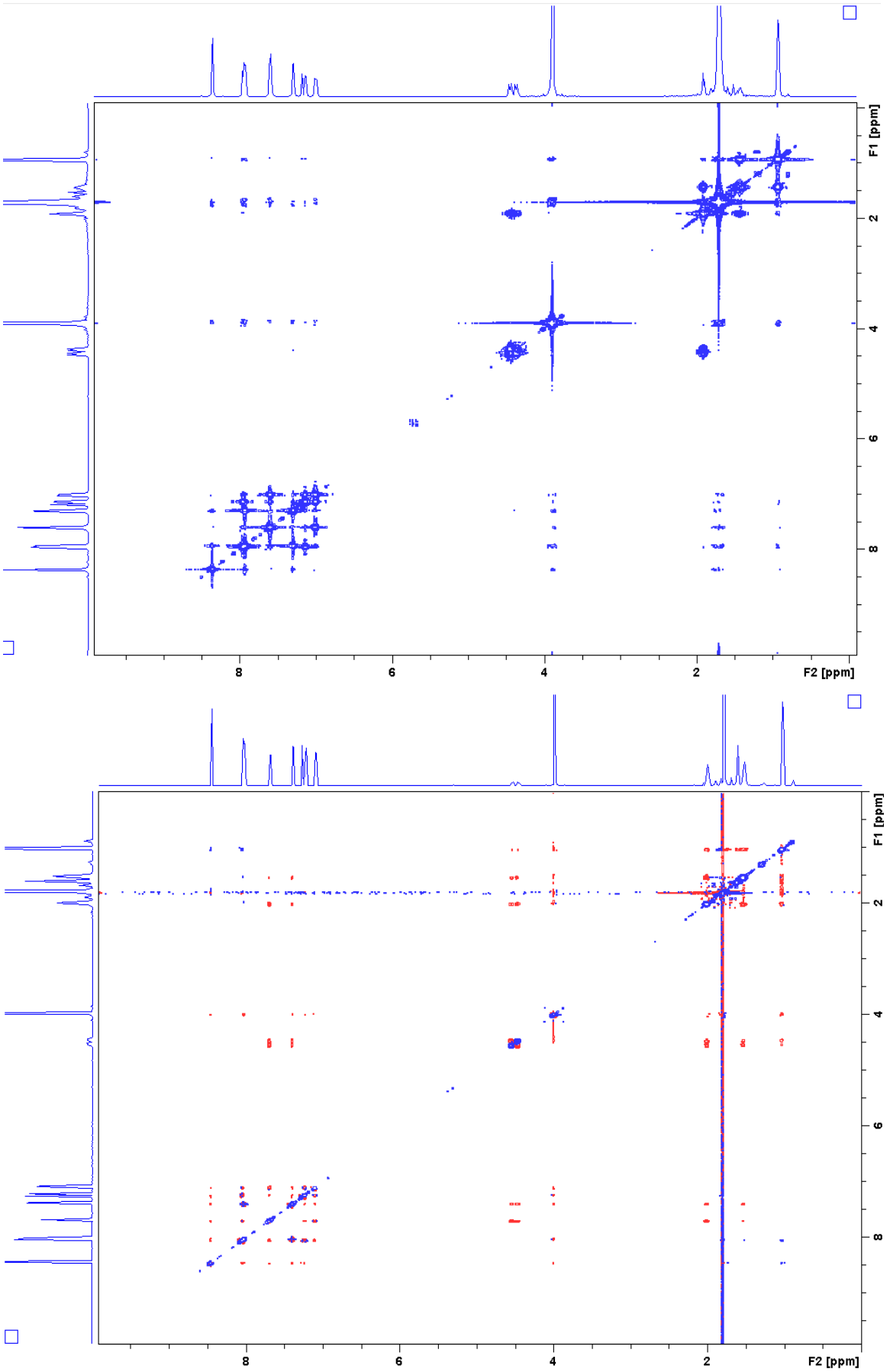

Figure S4. COSY and NOESY spectra for compound **4**.

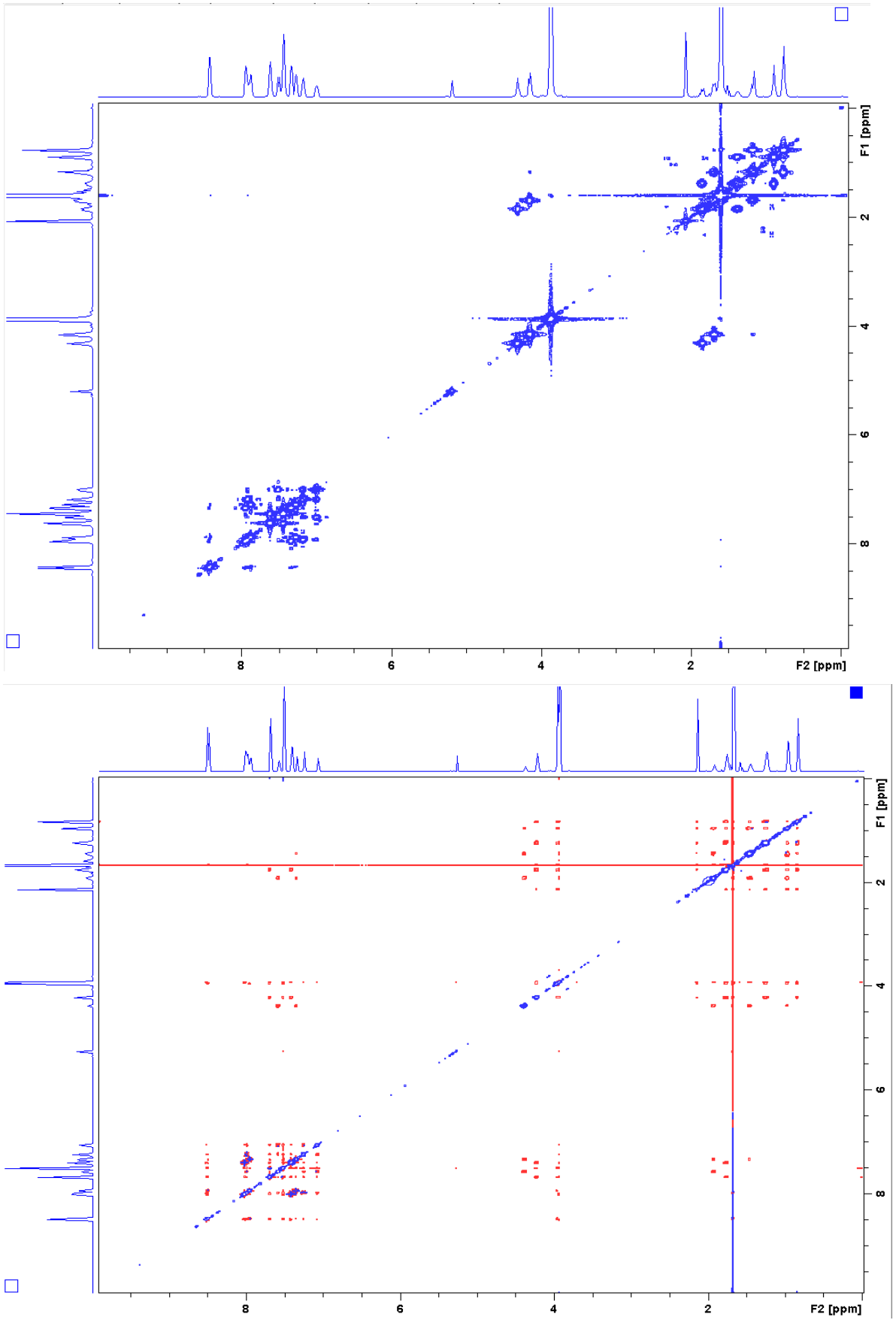

Figure S5. COSY and NOESY spectra for compound **5**.

Biological Application

Cell Line and Culture

The T47D human mammary adenocarcinoma and the human ovarian carcinoma (A2780 and A2780cis) cell lines were grown in RPMI-1640, while the human colon cancer (HT29) were grown in DMEM. In all cases the medium was supplemented with 10% (v/v) fetal bovine serum (FBS). Extra supplements of 0.2 unit/mL bovine insulin, 2 mM and 4 mM in L-glutamine was applied to the medium of the T47D, A2780 (and A2780cis) and HT29 cells, respectively. Cell growth was carried out in an atmosphere of 5% CO_2 at 37 °C. Due to low aqueous solubility, the test compounds were dissolved in DMSO first and then serially diluted in complete culture medium such that the effective DMSO content did not exceed 1%.

Cytotoxicity assay

Cell proliferation was evaluated by assay of crystal violet (T47D, A2780, A2780cis) or by the MTT, (3-(4,5-dimethylthiazol -2-yl)-2,5-diphenyltetrazolium bromide, method (HT29). T47D, A2780, A2780cis or HT29 plated in 96-well sterile plates at a density of 5×10^3 cells/well with −180 µL of medium and were then incubated for 48 h. After attachment to the culture surface the cells were incubated with various concentrations of the compounds tested freshly dissolved in DMSO and diluted in the culture medium by adding 20 µL (DMSO final concentration 1%) for 48 h at 37 ºC. When the crystal violet assay was employed, the cells were fixed by adding 10 µL of 11 % glutaraldehyde; then, the plates were stirred for 15 min at room temperature and then washed three-four times with distilled water; the cells were stained with 100 µL of 1 % crystal violet; subsequently, the plates were stirred for 15 min and then washed three-four times with distilled water and dried. 100 µL 10 % acetic acid were added and the plates were stirred for 15 min at room temperature. For the MTT assay (HT-29 cells), the medium was removed by pipetting, then 200 ul of DMEM medium and 50 uL of a MTT solution 5 mg/mL was added and left at 37 ºC (5% CO2, at dark) for 4 hours. Finally, this solution was removed from each plate, 100 µL of DMSO was added and left 5 minutes (always at dark) before measurement. Absorbance was measured at 595 nm and 560 nm for crystal violet and MTT assays, respectively, in a Tecan Ultra Evolution spectrophotometer.

The effects of complexes were expressed as corrected percentage inhibition values according to the following equation,

$$(\%)\ \text{inhibition} = [1 - (T/C)] \times 100$$

where T is the mean absorbance of the treated cells and C the mean absorbance in the controls.

The inhibitory potential of compounds was measured by calculating concentration-percentage inhibition curves, these curves were adjusted to the following equation:

$$E = E_{max}/[1 + (IC_{50})/C)^n]$$

were E is the percentage inhibition observed, E_{max} is the maximal effects, IC_{50} is the concentration that inhibits 50% of maximal growth, C is the concentration of compounds tested and n is the slope of the semi-logarithmic dose–response sigmoid curves. This non-linear fitting was performed using GraphPad Prism 2.01, 1996 software (GraphPad Software Inc.).

For comparison purposes, the cytotoxicity of cisplatin was evaluated under the same experimental conditions. All compounds were tested in two independent studies with triplicate points. The in vitro studies were performed in the USEF platform of the University of Santiago de Compostela (Spain) and in the SACE service from the University of Murcia for HT-29 cell lines.

All studies were performed with maximum DMSO concentration of 1% (except for cisplatin) and in all the experiments measurements were corrected with a DMSO-water control, and observed a growing inhibition of 6-8% compares to a control where cells are in normal growing media.

Cell cycle arrest assays

Cell cycle arrest studies were performed on HT-29 colon cancer cells. Typically, 1.5 x 10^5 cells were seeded in a 6-well plate with DMEM medium (5 mL/plate). Cells were allowed to fix to the plate by incubation for 24 hours at 37 ºC (5% CO_2). Then, the compounds **3**, **4**, and **5** were added at final concentrations coincident with their respective IC_{50} values in the different plates. Two plates were untreated, for being used as a blank (without any posterior treatment of any dye) and as a control. The cultures were incubated for other additional 48 h in the same conditions as described above. At this point, the medium was removed and stored in 15 mL falcons. Immediately, the fixed cells were treated with 1 mL of tripsine for 4 minutes at 37 ºC and then 1 mL of DMEM medium containing FBS was added to stop the enzymatic action. The resulting 2 mL were added to the 15 mL falcon. In this way both possible floating cells and adherent cells were considered for the assay. Cells were centrifugated (200 g, 10 minutes) and the precipitated (cells) were washed with 2 mL of PBS. After another centrifugation (same conditions) and removing the supernatant, cells were resuspended in 200 µL of PBS. Then, 2 mL of a PBS/ethanol mix solution (70/30) was added to the cells. The solution was kept in ice for 30 minutes. The supernatant was eliminated by centrifugation (same conditions). The cells were again resuspended with 800 µL of PBS: Finally, 100 µl of a RNase solution (1 mg/mL) and 100 µL of a propidium iodide solution (400 µg/mL) were added. After stirring the resulting suspension was incubated at 37 ºC for 30 minutes at dark. Stained cells were then analyzed in a Becton-Dickinson FACScalibur flow cytometer.

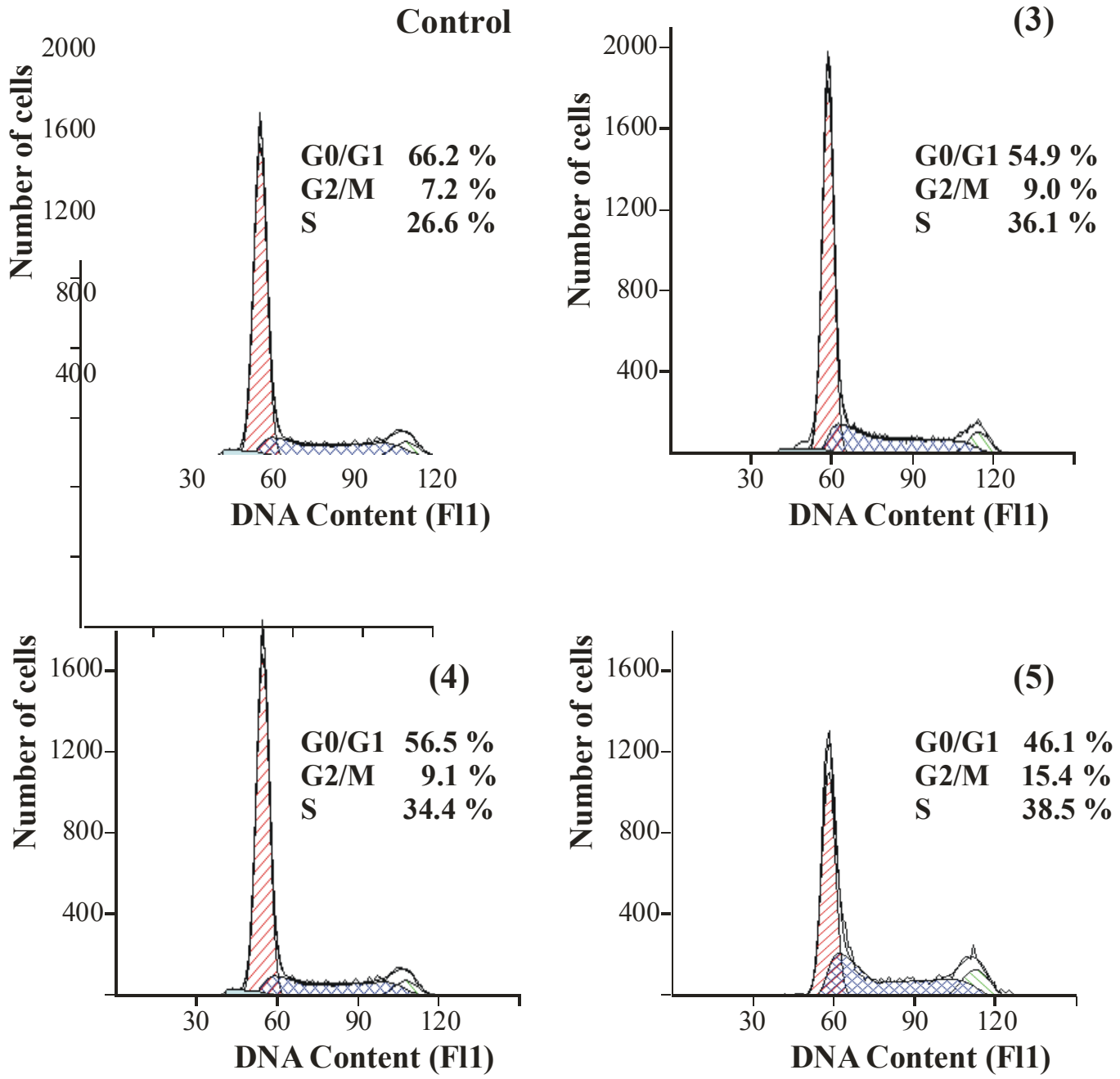

Figure S6. Cell cycle arrest results. Integrated areas and fit with the ModFitLT package are printed under the experimental curve. Percentages for each phase of the cell cycle are given in each figure. Number of control cells wer *ca.* double to that obtained for the other assays: its Y-axis has been re-scaled.

Apoptosis Experiments

For apoptosis determination assays, 10^5 cells were typically seeded in a 6-well plate. HT-29 cells without (blank and control) and with compounds were incubated, collected and washed once with PBS as described above (no PBS/ethanol mix was used in this case). After removing the PBS, 100 µL of a

solution containing Annexin V and IP (Annexin-V-Fluos from Roche) was added to the cell pellet. Cells were resuspended in this solution and leave at room temperature and at dark for 15 minutes. 200 µL of PBS was added immediately previous to the measurements. These were carried out in a Beckman Coulter Epics XL flow cytometer, registering the emission at wavelengths of 620 and 525 nm for IP and Annexin V, respectively. In eache case, 10000 events were acquired.

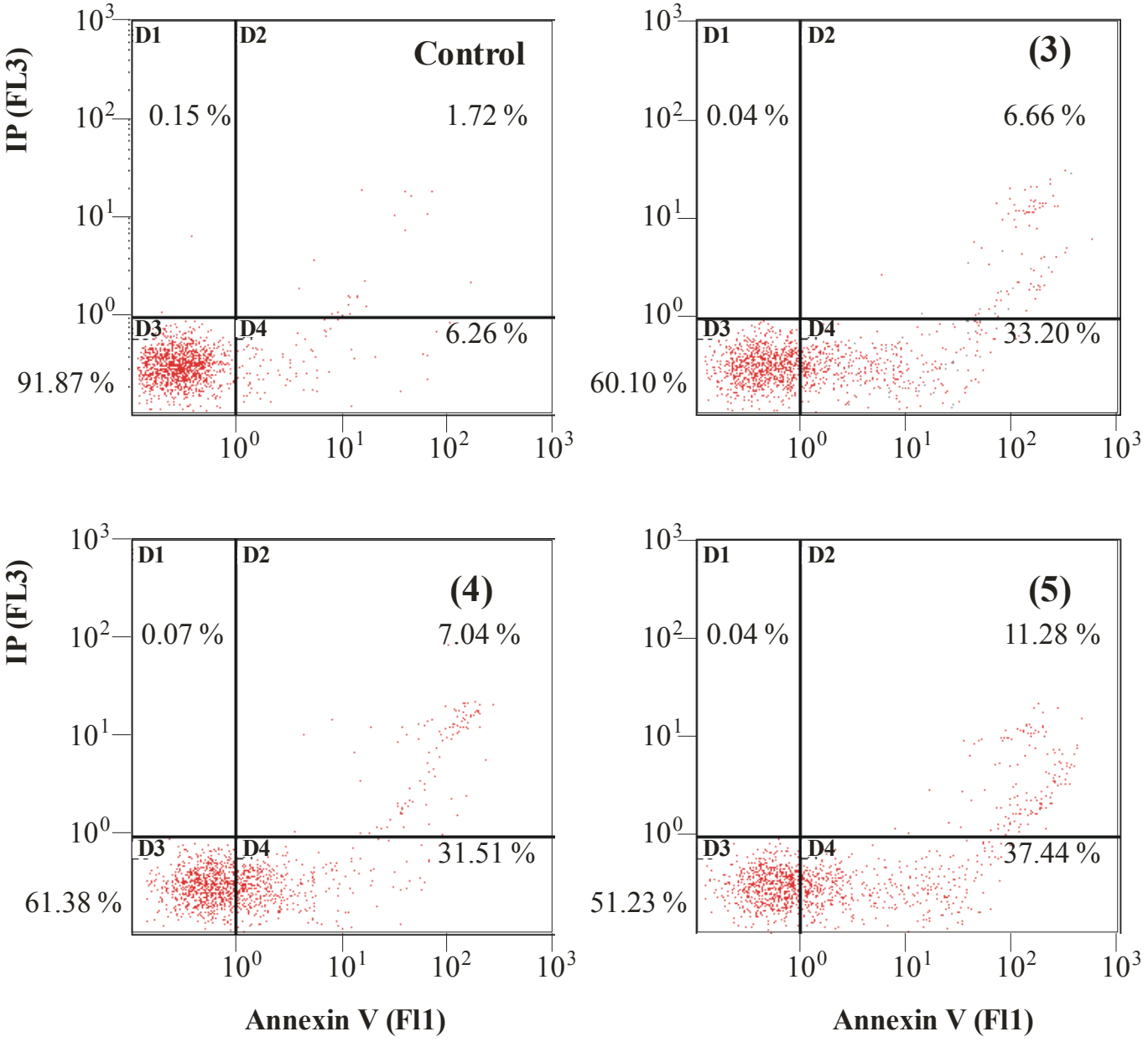

Figure S7. Results of the flow cytometric assays with Annexin V and propidium iodide The four typical quadrants identifying the necrotic (upper left quadrant D1, only IP stained cells), the late apoptotic (upper right quadrant D2, cells stained with both fluorescent dyes), the living (lower left quadrant D3, not or low

stained cells), and early apoptotic (lower right quadrant D4, only the annexin-V stained cells) cells appear in these diagrams. The percentage of the number of cells for each quadrant is indicated in the text.

Metal Cellular Accumulation Studies

Tumour cells plated in a 12-wells cell culture plate at a density of 750000 cells/well and maintained at 37ºC in a 5% CO_2 atmosphere. Compounds to 20 μM were added to cells for 48h, after this time cells were detached from the plate by using EDTA-Trypsin. The cell suspension from each well was transferred to eppendorf tubes and centrifuged 400 g for 5 min at room temperature. The supernatant was discarded and pellet was suspended in cell culture medium and washed by two additional centrifugations. The final pellet was resuspended in 0.5 ml pure HNO_3 and diluted to 5 ml milliQ water for analysis ICP-MS. A Varian 820-MS inductively coupled plasma-mass spectrometer was used to determine Ir, Ru and Rh concentration. Samples were introduced via a concentric glass nebulizer with a free aspiration rate of 1 mL/min, a Peltier-cooled double pass glass spray chamber, and a quartz torch. A peristaltic pump carried samples from a SPS3 autosampler (Varian) to the nebulizer. Ir standards were prepared by serial dilution of a solution containing 1000 mg/L of Ir in 5% HCl (Trace Cert. Fluka), 1000 mg/L Rh and 1000 mg/L Ru (Panreac). A nine-point calibration curve was made over a concentration range of 0.1-100 mg/L Ru and Rh and 1-100 mg/L Ir. ^{193}Ir, ^{101}Ru and ^{103}Rh were monitored, and ^{159}Tb and ^{105}Pd were used as internal standards. Data acquisition was done using peak hopping with a dwell time of 30 ms, 60 scans/replicate, and three replicates per sample from two independent experiments.

HSA Interaction Study

Table S3. Quenching and Binding Parameters for the interaction of complex **4** with HSA, HSA-WF and HSA-DG.

Study[a]	T(K)	10^{-4} K_{SV}[a] (M^{-1})	R[a]	10^{-4} K_A (M^{-1})	η
HSA	298	3.33	0.9979	6.46	1.13
HSA-WF	298	3.85	0.9989	5.69	1.54
HSA-DG	298	2.82	0.9808	4.14	1.38

[a] Calculated using only the data in the linear range.

For improved design of next-generation drug candidates, researchers are interested in deeper insight into the binding sites of metallodrugs on biomolecules. To identify the binding site location of benzimidazole metal complexes on the region of HSA, competitive binding experiments were carried out using warfarin (WF), a characteristic marker for site I and dansyl glycin (DG) as one for site II.[14] The weak fluorescence intensity of warfarin is enhanced upon binding with HSA because of its interaction with Trp 214 in HSA when excited at 320 nm. The fluorescence intensity of warfarin, in its bound state to HSA, decreases if a second ligand competes for the site occupied by it. Complex **4** binding site has evaluated by monitoring the changes in the fluorescence spectra of gradual increase in concentration of complex **4** in HSA-WF solution. Figure 4B depicts a decrease in the emission intensity of HSA−WF (in the wavelength region of 348−450 nm, excited at 320 nm) when complex **4** is added. The quenching of warfarin bound to protein upon addition of **4** reflects a reduction in the warfarin binding capacity at the binding site of HSA and preferential accessibility of Trp 214 in HSA by **4**. Therefore it is very likely that the **4** binding occurs at the warfarin site I. With similar experiments, regular decrease in fluorescence intensities of HSA-DG with increasing concentration of the complex **4**, indicating the binding of complex to the protein at the dansyl glycin site II. Supporting Information (Figure S10) shows the plots of log (F_0 − F)/F versus log {1/([Q_t] − (F_0− F)[P_t]/F_0)} for the interaction between HSA and complex **4**. K_A, η and K_{SV} obtained from the plots are listed in Table S3.

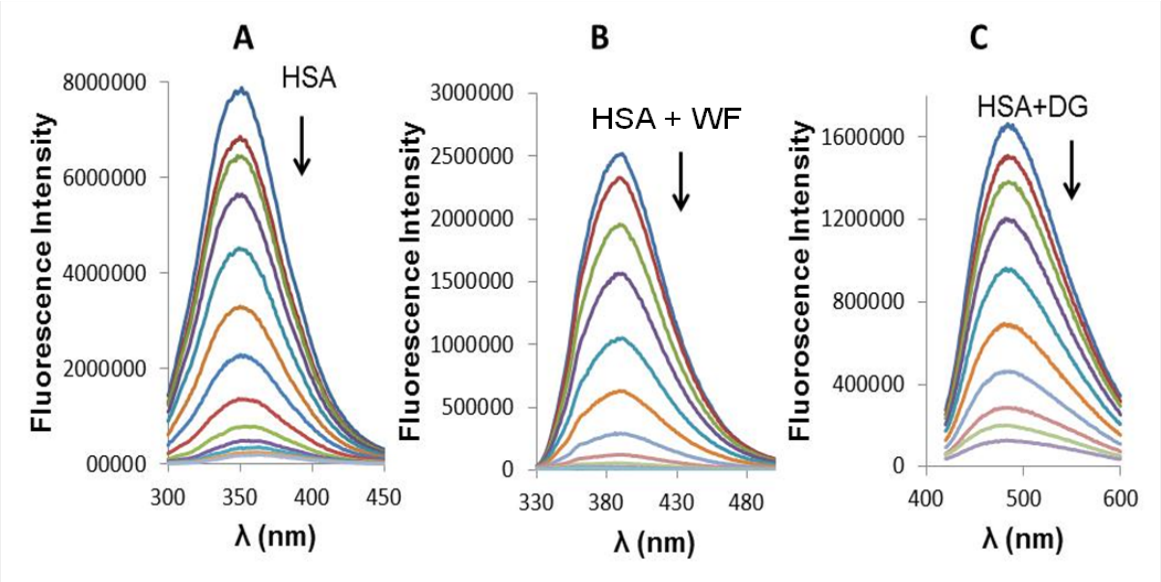

Figure S8. Emission spectra of HSA, HSA-WF and HSA-DG in presence of increasing amounts of complex **4**. λex = 295 nm, [HSA] = 5.1 µM; λex = 295 nm, [HSA-WF] = 5.0: 5.0 µM; λex = 295 nm, [HSA-DG] = 5.0: 5.0 µM; [Complex 4] : 0-50 µM (top to bottom gradual increments). 296 K. pH = 7.4.

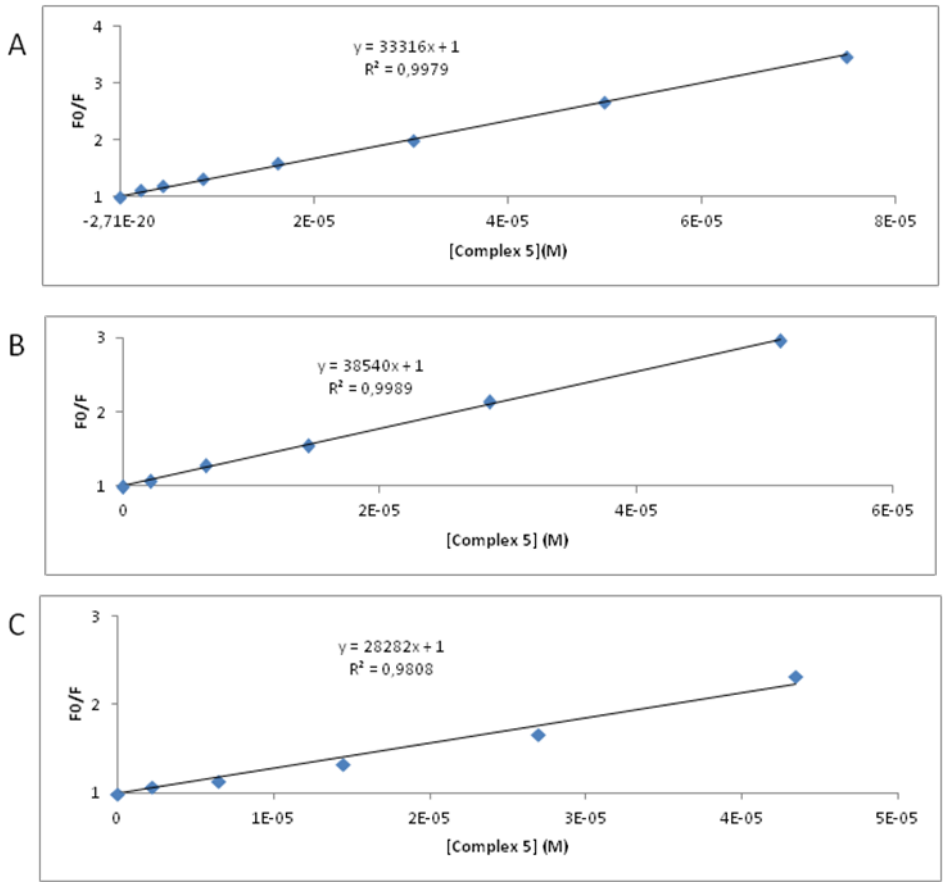

Figure S9. The Stern- Volmer quenching plots of A) HSA, B) HSA-WR and C) HSA-DG in presence of complex **4**.

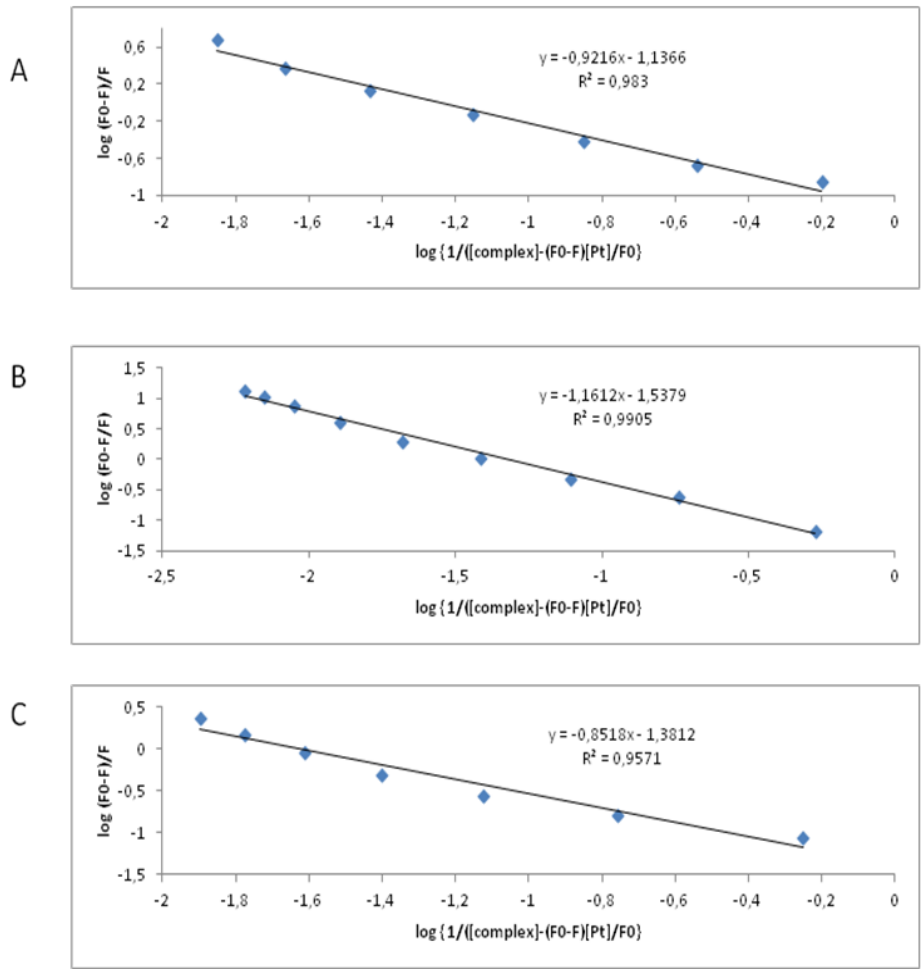

Figure S10. Plots of log(F0-F)/F versus log {1/([Qt] – (F0 -F) [Pt]/F0)} for A) HSA, B) HSA-WR and C) HSA-DG in presence of complex **4**.

Interaction with DNA

To investigate the binding mode between the new metal complexes and DNA, fluorescence competition experiments with Hoechst 33258 were employed. Hoechst 33258 binds to DNA in two concentration dependent ways. The first type of binding occurs in the minor groove at low dye-to DNA ratios. The fluorescence yield of Hoechst 33258 increases significantly in presence of DNA. The displacement of bound Hoechst 33258 from its binding site on ct-DNA is implicated from a decrease in its fluorescence intensity on addition of the complex **4**. When the complex is added to Hoechst-DNA solution we observed a decrease (~81%) in the fluorescence (Supporting Information Figure S11). This suggests that especially complex **4** capable of binding in the minor groove of DNA.

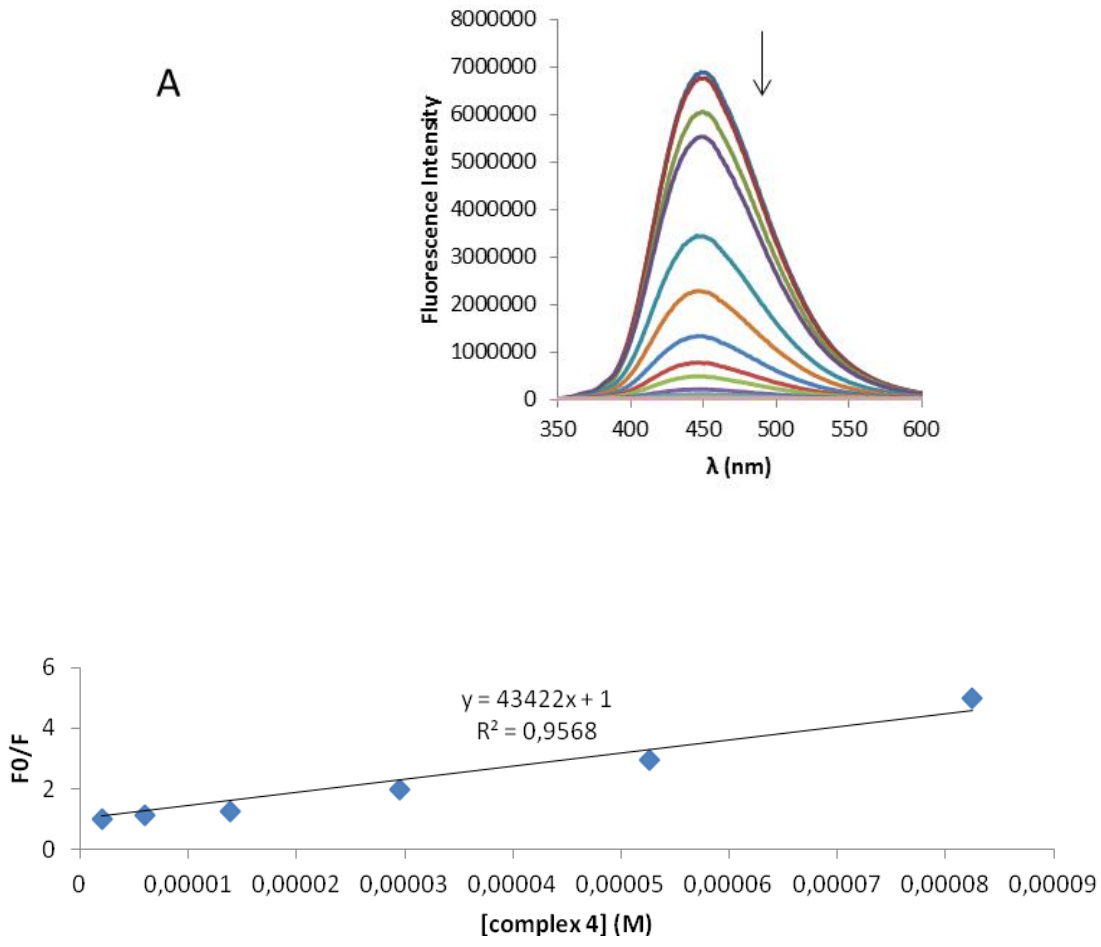

Figure S11. A) Changes in fluorescence spectra of Hoechst -ctDNA in presence of increasing amounts of complex 4. λex = 450 nm, [DNA] = 10 µM; [Complex **4**] : 0-150 µM (top to bottom gradual increments). Temperature = 296 K. B) The Stern-Volmer quenching plots of Hoechst bound ctDNA in presence of complex **4**.

Electrophoretic Mobility Study

The influence of the compounds on the tertiary structure of DNA was determined by their ability to modify the electrophoretic mobility of the covalently closed circular (ccc) and open (oc) forms of pB*R*322 plasmid DNA. The compounds **2**−**11** were incubated at the molar ratio r_i =0.50 with pB*R*322 plasmid DNA at 37 °C for 24h. Representative gel obtained for the new compounds **2**−**11** are shown in Figure S12. The behavior of the gel electrophoretic mobility of both forms, ccc and oc, of pB*R*322 plasmid and DNA:cisplatin adducts is consistent with previous reports. Noteworthy, the free benzimidazole ligands and their metal complexes **2**−**11** do not seem to cause important conformational changes of DNA at these conditions.

Experimental conditions:

pB*R*322 plasmid DNA of 0.25 μg/μL concentration was used for the experiments. Four microlitres of charge maker (Lambda–pUC Mix marker, 4) were added to aliquots parts of 20 μL of the drug–DNA complex. The platinum complexes were incubated at the molar ratio r_i = 0.50 with pB*R*322 plasmid DNA at 37 ºC for 24 h. The mixtures underwent electrophoresis in agarose gel 1% in 1 × TBE buffer (45 mM Tris-borate, 1 mM EDTA, pH 8.0) for 5 h at 30 V. Gel was subsequently stained in the same buffer containing ethidium bromide (EB) (1 μg/mL) for 20 min. The DNA bands were visualized with an AlphaImager EC (Alpha Innotech).

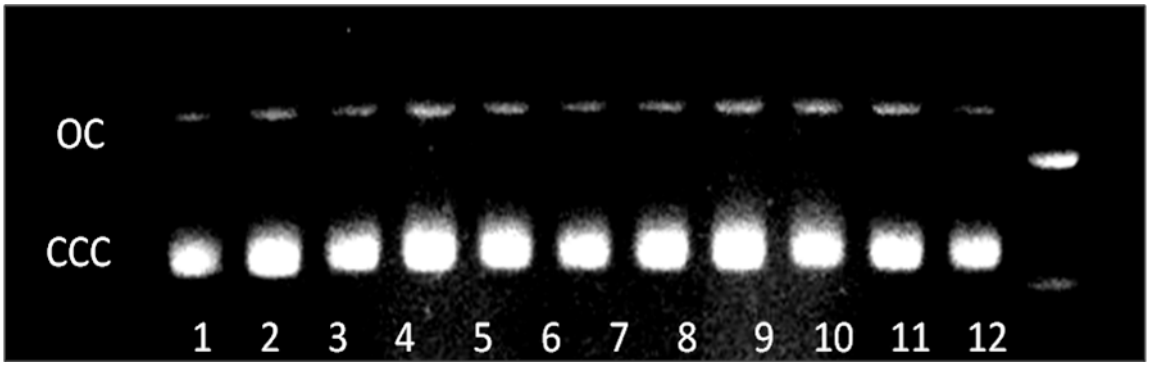

Figure S12. Electrophoretic mobility pattern of pB*R*322 plasmid DNA incubated with the ligands and their metal complexes: lane 1, CDDP; lane 2-11, compounds 2-11; lane 12, pBR322.

Electrophoretic mobility of compound 3 with different ratio with DNA:

For more investigation, we now carried out gel electrophoresis of compound **3** with pBR322 plasmid at different ratio considering "Metal complex-DNA ratio could be key factor for plasmid mobility assay".

Complex 3 incubated with pBR322 plasmid DNA at molar ratio 5.0, 2.0, 1.0. 0.5, 0.2, 0.1, 0.05, 0.02, 0.01, 0.005 and 0.002 at 37 ºC for 24 h. The electrophoresis is carried out with similar conditions as stated above. However, compound didn't modified structure of pBR322 plasmid at any molar ratio. These results coincide with our earlier results of electrophoresis (Ref. 7a). At the end, we can only conclude that compounds are able to bind with minor groove weakly as resulted from fluorescence competition experiments. However, these complexes are not able to modify structure of pBR322 plasmid under studied conditions.

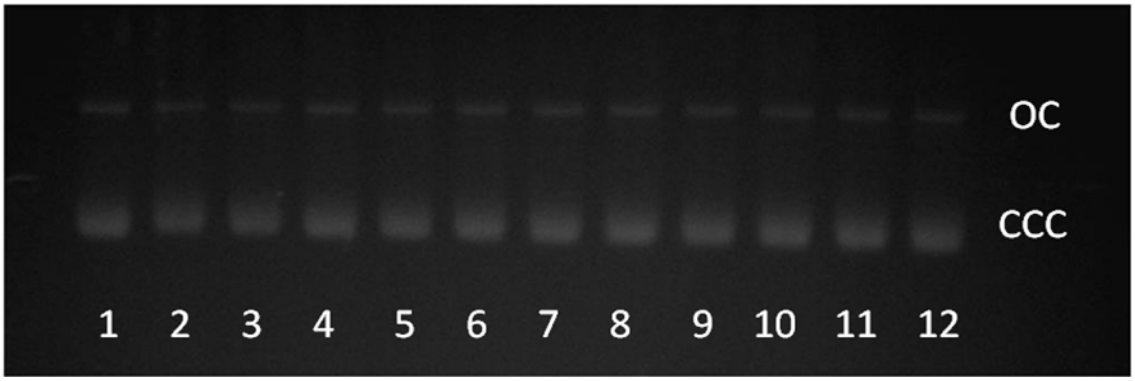

Figure S13: Electrophoretic mobility pattern of pB*R*322 plasmid DNA incubated with the complex **3**: lane 1, pBR322; lane 2-12, compound 3-DNA ratio 5.0, 2.0, 1.0. 0.5, 0.2, 0.1, 0.05, 0.02, 0.01, 0.005 and 0.002 respectively.

References:

[i] Apex2, Data Collection Program for the CCD Area-Detector System; SAINT, Data Reduction and Frame Integration Program for the CCD Area-Detector System. Bruker Analytical X-ray Systems, Madison, Wisconsin, USA, 1997-2006.

[ii] G. Sheldrick, Program SADABS: Area-detector absorption correction, University of Göttingen, Germany, 1996.

[iii] G. M. Sheldrick, *Acta Crystallogr. A*, 2008, *64*, 112-122.

[iv] K. Brandenburg, Diamond (Version 3.2), Crystal and Molecular Structure Visualization, Crystal Impact – K. Brandenburg & H. Putz Gbr, Bonn (Germany) 2009.

[v] (a) H.D. Flack, M Sadki, A.L. Thompson, D.J. Watkin, Acta Crystallogr. Sect. A, 2011, *67*, 21; (b) H.D. Flack, G. Bernardinelli, Chirality 2008, *20*, 681; (c) H.D. Flack, G. Bernardinelli, Acta Crystallogr. Sect. A 1999, *55*, 908; (d) H.D. Flack, Acta Crystallogr. Sect. A 1983, *39*, 876.